ChemPubSoc Europe

DOI: 10.1002/celc.201700699

CHEMELECTROCHEM Articles

High-Stability Electrodes for High-Temperature Proton Exchange Membrane Fuel Cells by Using Advanced Nanocarbonaceous Materials

Héctor Zamora,[a] Jorge Plaza,[a] Pablo Cañizares,[a] Manuel A. Rodrigo,[a] and Justo Lobato*[a]

This work studies the stability and performance of a cathodic electrode for high-temperature proton exchange membrane (HT-PEMFC) systems prepared with a carbon nanosphere (CNS) based microporous layer and carbon nanofibers (CNFp) used as a catalyst support. The obtained results are compared with a standard Vulcan carbon XC72 based electrode. With this purpose, two membrane–electrode assemblies (MEAs) were prepared using the cathodic electrodes and tested in a 25 cm^2 HT-PEMFC system. Preliminary short-life tests around 330 h were carried out with both MEAs. During the tests, different characterization procedures, consisting of polarization curves, spectroscopy impedance analysis, cyclic voltammetry and linear sweep voltammetry were performed in order to evaluate the evolution of the main stability and performance parameters of the MEAs. Results showed that the application of these new materials increases positively the stability of the MEA in comparison with the standard Vulcan carbon XC72 material, with a negligible decrease in the performance of the advanced MEA during all tests, making these results very promising to overcome the service lifetime limitations of these systems.

1. Introduction

Nowadays, the proton exchange membrane fuel cell (PEMFC) technology has been demonstrated as a strong alternative to substitute traditional non-renewable energy sources.[1–3] These electrochemical devices use hydrogen to generate electrical energy, producing water as product, which make them very environmental-friendly processes.[4,5] Concretely, the high temperature PEMFCs have received much attention in the last years, since the high temperature provides many benefits respect to low temperature fuel cell devices, such as the improvement of water and heat management, and specially, the better tolerance of the platinum catalyst to the presence of poisoning agents contained in the hydrogen flow.[6–8] Carbon black materials, especially Vulcan Carbon, are the typical material used in the manufacturing of the microporous and catalytic layers, due to their good physicochemical and electrochemical properties (such as high surface area, adequate porosity distribution, good electrical conductivity, and acceptable thermal stability), and easy-availability at low cost. However, in terms of durability, this material exhibits important disadvantages related to its poor electrochemical and chemical resistance in the aggressive operational conditions of the HT-PEMFC. These harsh conditions are given due to the polibenzimidazole (PBI) based membranes (typical membranes used in HT-PEMFC) must be doped with phosphoric acid in order to get acceptable protonic condition, and this acid, combined with the high temperature operational range, performs a strong degradation on the Vulcan carbon based electrode components.[9–11] Furthermore, the electrochemical carbon corrosion starts to appear at potentials over 0.267 V vs RHE, resulting in a several corrosion at voltages over 1.2 V. These voltage values are easily achieved during the turn-on and shut-down processes during the fuel cell operation, and also in open circuit voltage (OCV) conditions.[2,10] The degradation of the Vulcan carbon carries out some problems related with the performance and durability of the fuel cell (mass transfer limitation, migration and agglomeration of the platinum particles, or the increasing of the ohmic resistance of the electrodes, due to the degradation of the carbonaceous structure of the electrode). All these facts have a negative impact on the performance of the MEA.[11–13]

Considerable research efforts have focused on the search of alternative materials to substitute the Vulcan carbon in the HT-PEMFC electrodes, especially in the catalyst support. It is well known that the catalyst support plays a very important role on the performance and above all the durability of PEMFC technology. Some of the target-required properties are: high electrical conductivity to assure the electron transfer, high surface area to provide a high dispersion of platinum nanoparticles, adequate gas permeability, in order to perform the correct diffusion of the reactive gases along all catalyst layer area, and good corrosion resistance under oxidizing conditions.[14] Moreover, the MPL provides some critical advantages to the fuel cell operation (higher stability, better gas distribution through the electrode surface and better management of the generated water in the cell),[15,16] and the degradation of this layer has a very important effect on the service lifetime of the electrode. Recently, some novel ceramic materials, especially different carbide materials based on Tungsten, Silicon or Titanium materials,[2,17–20] have been evaluated as catalyst support looking for an improvement service lifetime of the

[a] Dr. H. Zamora, J. Plaza, Prof. P. Cañizares, Dr. M. A. Rodrigo, J. Lobato
Chemical Engineering Department. University of Castilla-La Mancha
Enrique Costa Building, Av. Camilo Jose Cela 12
13004, Ciudad Real (Spain)
E-mail: Justo.lobato@uclm.es

catalytic layer. Results obtained are promising,[18,19] and they are related to their high electrochemical and thermochemical stability and the excellent mechanical properties.[19,20] However, their low surface area and conductivity in comparing with the Vulcan carbon materials reduce the performance of these non-carbonaceous based materials when they are used in HT-PEMFC systems. On the other hand, other advanced carbonaceous materials, such as carbon nanofibers, or graphene,[21–23] due to their high graphitic character, have been demonstrated higher stability than other carbonaceous materials against the electrochemical corrosion, and keep good values in terms of surface area or electrical conductivity.[22–25] In previous works carried out by our research group, carbon nanospheres and carbon nanofibers were preliminary evaluated to be used as MPL,[15] and these both advanced nanocarbonaceous materials demonstrated an improvement, in terms of stability, compared with the standard Vulcan carbon based electrodes during ex-situ electrochemical and thermochemical corrosion tests. Thus, in this work, two different nanocarbonaceous materials (Carbon nanospheres (CNSs) and Carbon nanofibers Platelet (CNFp) have been tested as raw materials to prepare the MPL and as catalyst support, respectively, in a cathodic electrode to be used in HT-PEMFC, with the objective to improve the durability of the MEAs used in these devices.

2. Results and Discussion

Figure 1 shows the evolution of the cell voltage with time during the tests carried out with the two MEAs prepared in this work. The negative time-values of x-axis correspond with the break-in period, which lasted approximately 70 h and that was carried out at 160 °C and 0.1 A cm^{-2}.

As it can be observed, during the break-in procedure, the standard MEA exhibits the best performance, with cell voltages around 40 mV over the optimized MEA prepared with CNSs as microporous layer and CNFp as catalyst support (CNSs/PtCNFp based MEA). It must be pointed out that the standard MEA exhibited a very stable break-in process after the first 10 hours, while the CNSs/PtCNFp MEA showed a continuous activation process, increasing its cell voltage in nearly 20 mV during this conditioning time.

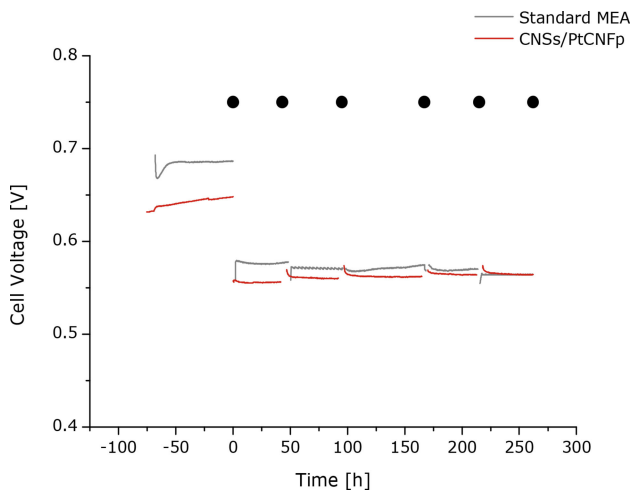

Figure 1. Evolution of the cell voltage of the different MEAs tested at constant $j = 0.3$ A cm^{-2} using pure H_2 ($\lambda = 1.5$) and O_2 ($\lambda = 9$) as fuel and oxidant, respectively. The negative time period corresponds to the break-in process, carried out at $j = 0.1$ A cm^{-2}. Black dots mark the different characterization tests performed on the MEAs during the preliminary life tests.

After the first characterization protocol, the current density was increased from 0.1 up to 0.3 A cm^{-2}, and this value was kept constant until the end of the tests.

It must be remarked that the standard MEA showed a better performance in terms of cell voltage during the first 180 hours of experiment, but then, the cell voltage of the two MEAs evaluated becomes closer and closer. In the last 40 hours of the life tests, the comparison reverses, and the fuel cell equipped with the CNSs/PtCNFp MEA started to overcome the fuel cell equipped with the standard MEA. It must be pointed out that among the different reached steady states, the CNSs/PtCNFp based MEA did not show any signs of degradation. Thus, after 262 hours, the standard MEA reached an average voltage drop value of -46.5 μV h^{-1}, while the optimized MEA showed an average activation rate of $+27$ μV h^{-1}. The improvement in the performance of the fuel cell equipped with the novel carbonaceous materials could be explained by a sort of positive effect of the harsh operation conditions, which in turn, produce a slight degradation on the CNFp support, increasing the porosity of this material and improving the gas diffusion through the electrode with time. At the same time, the MPL with CNSs avoids the Pt migration over the catalytic layer, which could explain the enhanced performance and stability observed in this experiment. Thus, despite the conventional Vulcan carbon based MEA shows a better cell voltage during the most time of the life test, the CNSs/PtCNFp based MEA outperforms it in terms of a negligible degradation rate, finally overcoming its performance.

Figure 2 shows the polarization curves measured at the beginning of the tests carried out with the MEAs, when the fuel cells were fed with oxygen and air. The obtained results are in agreement with the results shown in Figure 1. At low current densities (lower than 0.1 A cm^{-2}), the optimized MEA showed similar OCV values and performances working both with air and oxygen, while the standard MEA exhibited slightly higher performance working with oxygen.

It is also very noticeable that the standard MEA showed better performance at low and medium current densities (up to 0.4 A cm^{-2}), but within the high current density region, the optimized CNSs/PtCNFp based MEA overcame the performance of the standard one. The higher maximum power densities achieved by the optimized MEA respect to the standard one were around 15% higher when pure oxygen was used (303.3 mW cm^{-2} for CNS/PtCNFp MEA versus 280 mW cm^{-2} for the standard MEA at 0.7 A cm^{-2}, and 320.4 mW cm^{-2} for the optimized carbonaceous based MEA at 0.8 A cm^{-2}). When air was used, the standard MEA achieved higher power densities (165 mW cm^{-2} at 0.4 A cm^{-2}), but the values are closer to the CNSs/PtCNFp MEA (around 157 mW cm^{-2} at 0.4 A cm^{-2}).

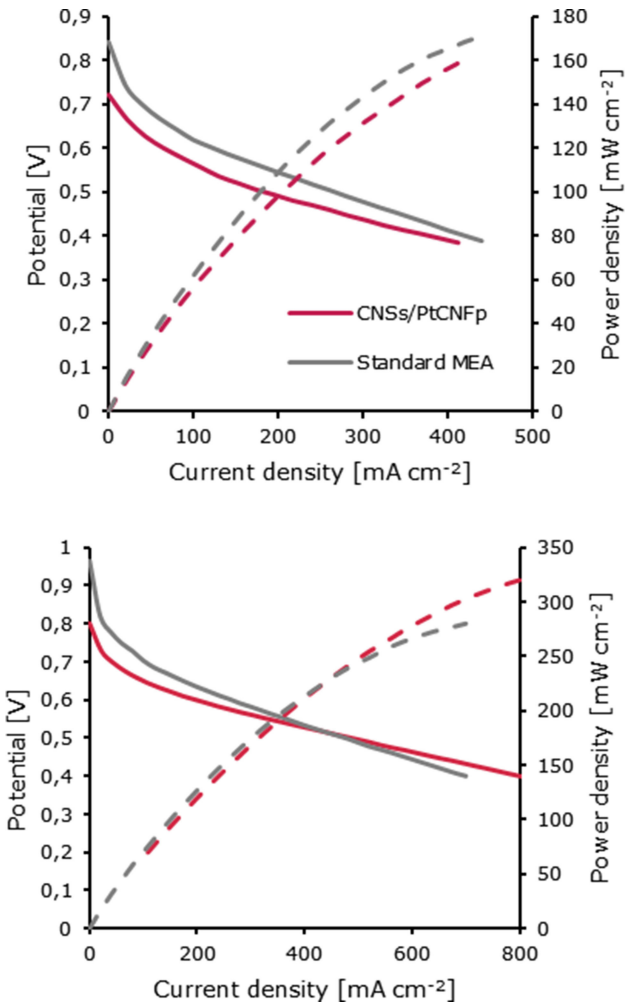

Figure 2. Comparison of the polarization curves obtained at t = 0 h for the MEAs tested. Top: Polarization curves performed with air. Bottom: Polarization curves performed with oxygen. Discontinuous lines correspond to the power density curves associated with them.

Figure 3 shows the evolution with time of the polarization curves performed to the both evaluated MEAs. As it can be observed, the evolution of the polarization curves is, again, in agreement to the previous results attained. On one hand, the CNSs/PtCNFp MEA exhibits a progressive and regular activation process during the test, increasing its performance among the different polarization curves performed with air and oxygen.

This improvement is especially remarkable at high current densities, for which the maximum power density achieved raised from around 320 mW cm^{-2} at the beginning of the short lifetest until 350 mW cm^{-2} at the end of the experiment. Both values are higher than the maximum values reached by the standard MEA (280 and 217 mW cm^{-2}, respectively).

Moreover, at low current densities (up to 0.3 A cm^{-2}) the standard MEA exhibits better performance than the CNSs/PtCNFp MEA, which explains the better cell voltage exhibited during the most part of the short test. However, in the last two polarization curves, a noticeable decrease in the performance of the standard MEA occurred. Moreover, the open circuit voltages did not suffer noticeable changes during the tests,

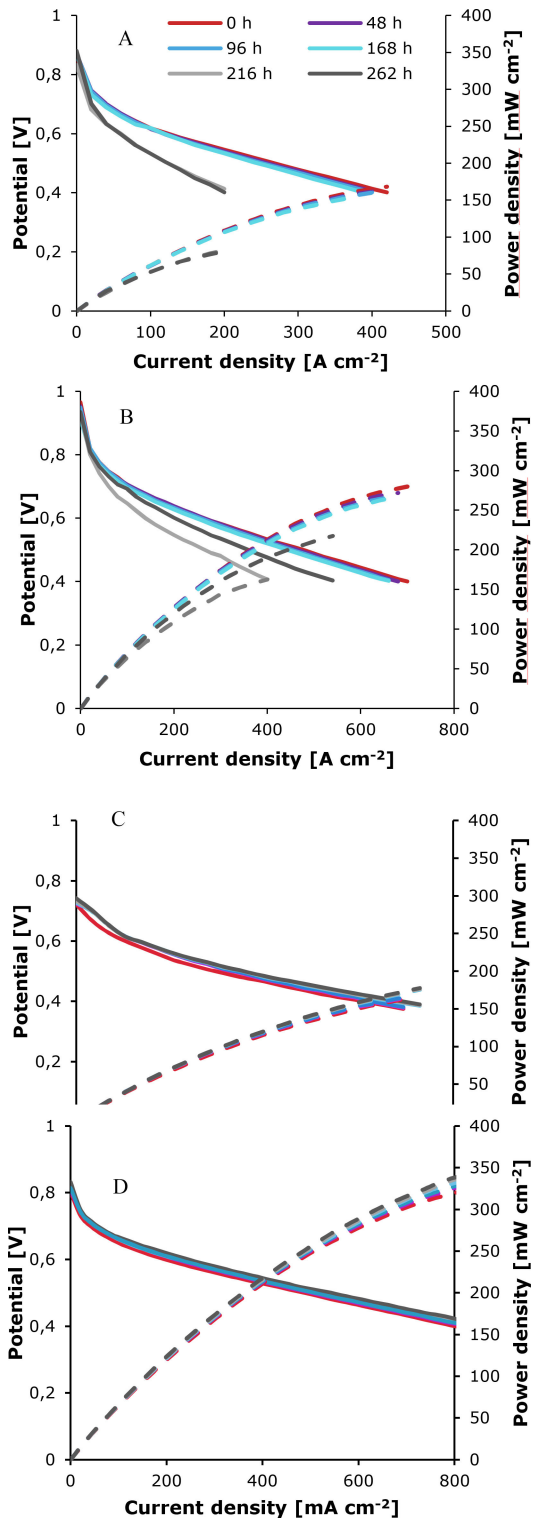

Figure 3. Evolution of the polarization curves performed along the different characterization test. Standard MEA running with air (A) and oxygen (B); CNSs/PtCNFp based MEA running with air (C) and oxygen (D).

which means that not important mechanical failures of the phosphoric acid doped PBI membranes occurred and, hence, the behavior of the MEAs should be explained only in terms of the degradation of the electrodes during the lifetest.[26]

In order to get more information about the behavior of the MEAs, Electrochemical Impedance Spectroscopy (EIS) at different current densities were carried out to the MEAs during the characterization protocols. Since the tendency of the evolution of the EIS through the different current densities was similar, it was decided to focus the study only on the analysis of the data obtained for the steady state current density (0.3 A cm^{-2}). Figure 4 shows the comparison between the starting impedance spectra obtained from the MEAs measured at 0.3 A cm^{-2} with air and oxygen. Likewise, Figure 5 shows the evolution of the impedance spectra at 0.3 A cm^{-2} performed with air and oxygen for the CNSs/PtCNFp based MEA. This Figure illustrates the way in which this spectra changes with time.

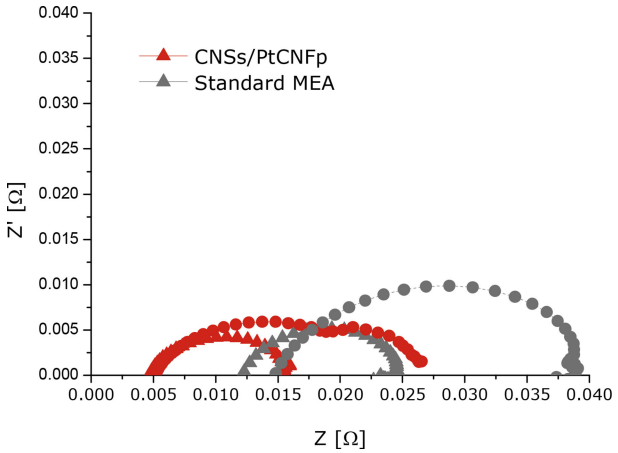

Figure 4. Impedance spectra measured at 0.3 A cm^{-2} for the different MEAs tested. Triangular symbols correspond to the data obtained for oxygen; circular dots correspond to data obtained in air.

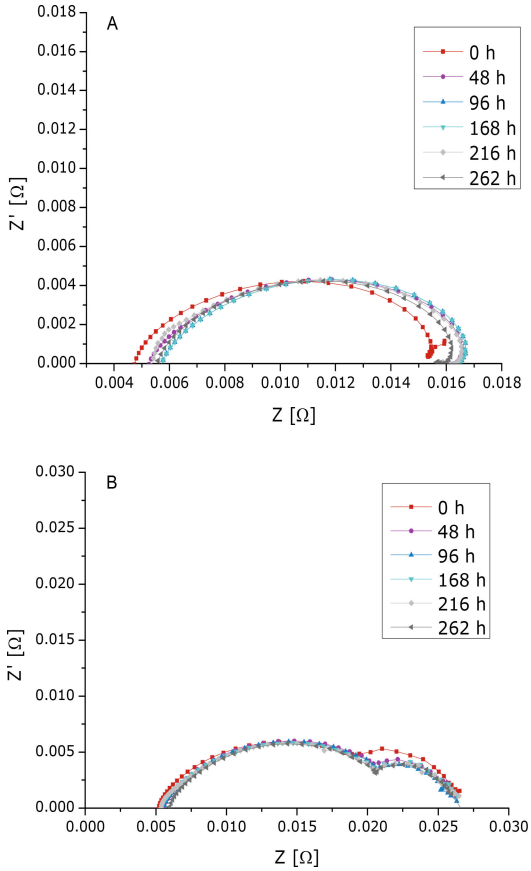

Figure 5. Evolution of the impedance spectra of the CNSs/PtCNFp based MEA. A) Evolution of EIS performed with oxygen as oxidant; B) with air as oxidant.

The spectra data obtained at j = 0.3 A cm^{-2} was fitted to an equivalent electrical circuit model R (RQ) (RQ).[26–29] From this fitting, ohmic resistance (R_Ω), charge transfer resistance (R_{CT}) and for the case of the impedances performed with air, the mass transfer resistances (R_{MT}) were obtained.[26–28] Their values are shown in Table 1.

R_Ω remained constant during all life tests, in values around 125 mΩ cm^2 for the case of the CNSs/PtCNFp MEA. This means that nor high degradation of the PBI membrane neither loss of conductivity (associated to drainage of phosphoric acid or the electrode degradation) occurred.[26]

Regarding to the standard MEA, the R_Ω value started in a higher value, around 200 mΩ cm^2 and after 262 hours, the value was increased until 260 mΩ cm^2, which suggests a degradation process on the electrodes or maybe a phosphoric acid leaching of the PBI membrane occurred during the last 60 hours of testing. Moreover, the optimized MEA exhibited closely similar values when comparing their R_Ω values obtained from

Table 1. Evolution of the different resistance parameters obtained from the impedance spectra data performed at j = 0.3 A cm^{-2}. All values are given in [mΩ cm^2].

Time		0 h			48 h			96 h		
MEA		R_Ω	R_{CT}	R_{MT}	R_Ω	R_{CT}	R_{MT}	R_Ω	R_{CT}	R_{MT}
CNSs/PtCNFp	Air	120.5	295.6	189.8	127.9	340.3	147.0	128.6	348.8	149.1
	Oxygen	111.1	245.1	0.0	121.2	259.7	0.0	129.7	255.7	0.0
Standard MEA	Air	278.9	449.8	29.6	216.4	447.9	45.4	210.6	420.5	46.3
	Oxygen	191.0	270.6	0.0	211.9	275.1	0.0	207.1	265.0	0.0
Time		168 h			216 h			262 h		
MEA		R_Ω	R_{CT}	R_{MT}	R_Ω	R_{CT}	R_{MT}	R_Ω	R_{CT}	R_{MT}
CNSs/PtCNFp	Air	124.2	347.7	143.1	124.6	350.4	125.6	137.1	337.1	132.5
	Oxygen	125.1	251.8	0.0	119.3	256.7	0.0	127.2	244.0	0.0
Standard MEA	Air	220.5	455.1	46.5	266.8	552.7	48.2	250.8	552.3	51.7
	Oxygen	221.1	279.0	0.0	262.2	560.8	0.0	247.5	385.9	0.0

air and oxygen spectra, respectively, at t = 0 h. This was expected, because this parameter is mainly affected by the ionic conductivity of the membrane, the electrical connection and the electrical resistance of the electrode and plates material.[26-28]

However, for the case of the standard MEA, a slight difference between this parameter calculated from the air and oxygen spectra at t = 0 hours can be observed, which could be explained in terms of a bad electrical connection, since the values obtained during the protocols are similar. If R_Ω values are compared between both MEAs, the standard one exhibited values higher than the optimized one. Furthermore, the activation process observed between the 216 and 262 hours could be attributed to the hydration of the membrane after a phosphoric acid leaching during this period of the life test.[30]

Moreover, The R_{CT} values, of the CNSs/PtCNFp based MEA and the standard one reached similar values during all lifetests, around 250 mΩ cm^2 with oxygen for both MEAs, being slightly higher for the standard one. This could help to explain the enhanced performance at high current densities of the CNSs/PtCNFp based MEA. When air was used as oxidant, the amplitude of the arc increased as compared to the impedances performed with pure oxygen, as it was expected due to the lower oxygen concentration. The highest increase on this parameter was obtained for the standard MEA, which means that the activation of the commercial Pt/Vulcan catalyst suffers a slower activation process using air than the lab-made CNFp catalyst used in the optimized MEA. Regarding to the evolution of this parameter with time, the CNSs/PtCNFp based MEA showed a slight increasing during the first 48 hours, and then, the value remained constant until the end of the lifetest, with an average value around 350 mΩ cm^2. On the other hand, the standard MEA exhibits values around 450 mΩ cm^2 during the first 200 hours, and then undergoes an increase in the value up to 550 mΩ cm^2. This fact is also observed running with air, which explains the strange decreasing of the performance of the MEA and it could be due to the degradation of the electrode, in addition to the decrease in the doping level of the PBI membrane during the last 60 hours of the test.

Finally, when air is used as oxidant, it can be observed that another small arc appears in all cases, due to the mass transfer limitations, which may be related to the porosity of the electrode. As it can be observed in Figure 4 and Table 1, this value is negligible for the standard MEA, which means that the porosity of the MPL and catalytic layer is good, and allows a good dispersion of the gas through all the electrode surface. The highest value is provided by the CNSs/Pt CNFp based MEA. As it was shown in previous works carried out by our research group,[31] the carbon nanofibers provide a highly compact appearance on the layers prepared with them. Thus, the high value of this parameter, as compared with the other MEAs tested, may be attributed to the catalytic layer, and could explain the lower performance of this MEA during the first hours as compared with the standard one, even if the standard MEA presents worse catalytic activity. It can also help to explain the gradual activation of the optimized MEA, since a small degradation of the CNFp based catalytic layer could increase its porosity, and this increase, in turn, can help to raise the gas diffusion and the performance as well. This fact is in agreement with the evolution of this parameter with time, shown in Table 1.

Figure 6 shows the evolution of the shape of the voltammograms obtained for the CNSs/PtCNFp and standard based MEAs

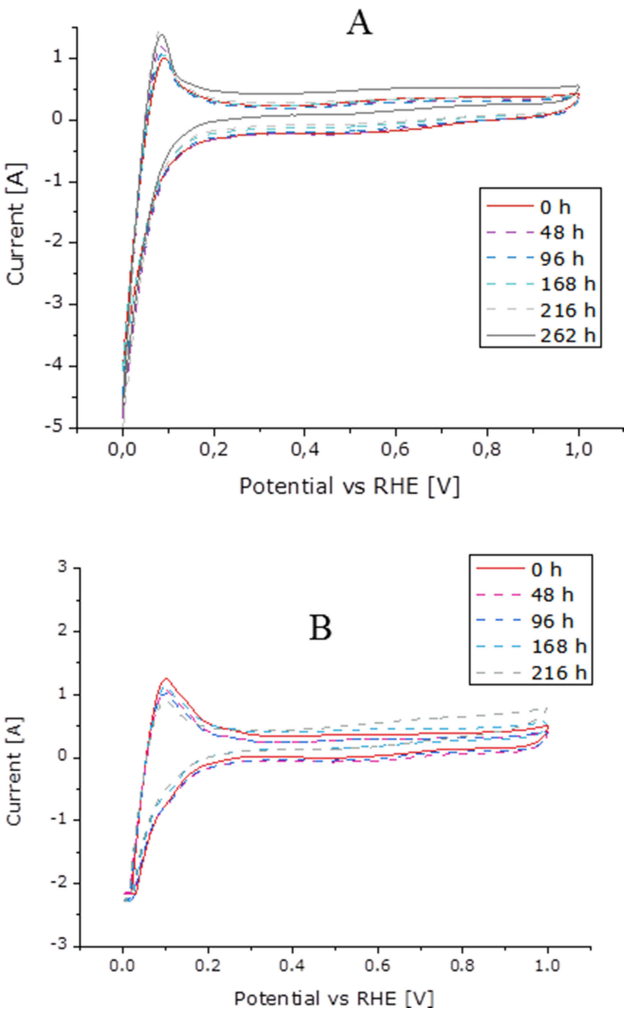

Figure 6. Evolution of the voltammograms with time for A) the CNSs/PtCNFp based MEA and B) the standard MEA.

during the different characterization protocols performed during the short life tests. As it can be observed, the standard MEA exhibits the largest ECSA value at the beginning of the life test, around 40% higher than the CNSs/CNFp based MEA. Regarding to the standard MEA test, during the last test an abnormal shape on the voltammogram was observed, so it was decided to remove it from the Figure 6B. At the end of the life test, it was asseverated that this strange shape occurred due to the mechanical failure and breakage of the PBI membrane, which could explain this fact was due to the crossover. Fortunately, since this was the last test of the experiment, this fact did not have any influence on the performance of the MEA shown during all life test.

Finally, Figure 7 shows the evolution of the ECSA values performed during the tests. As it can be observed, the

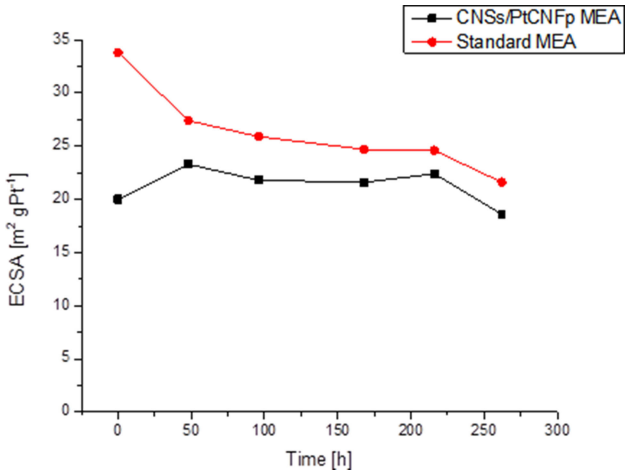

Figure 7. Evolution of the ECSA of the two MEAs tested over the course of 262 h.

optimized carbonaceous based MEA undergoes an increase of the ECSA value with time during the first 200 hours. Furthermore, if the starting and ending ECSA values are compared for this MEA, the ECSA degradation was lower than 7%, much lower than the degradation of the standard MEA, which was around 36%. Furthermore, ECSA values reached by both MEAs after 200 hours of lifetest are closely similar, which means that the starting higher ECSA value exhibited by the standard one does not become a critical advantage with respect to that obtained with the CNSs/PtCNFp based MEA.

3. Conclusions

The main conclusions that can be drawn from the results obtained in this work are the following:

- The MEA prepared with the nanocarbonaceous materials (CNS as MPL and Pt/CNFp as catalyst) exhibited a high stability, which make these materials a very promising candidates to substitute the Vulcan carbon XC72 in HT-PEMFC technology based on PBI membranes.
- The usage of advanced nanocarbonaceous materials decreases the ohmic and charge transfer resistance of the MEA respect to the standard Vulcan carbon based one.
- The stability of the catalytic layer, in terms of ECSA, is much higher with the new nanocarbonaceous materials.
- The optimization of the composition of the catalyst layer is required to optimize the performance of the Pt/CNFp as cathodic catalyst for these systems.

Experimental Section

Carbon nanospheres and carbon nanofibers were manufactured in our facilities, according to the procedure shown in literature.[24,25] Physicochemical properties of the CNSs can be found in a previous research study carried out by us.[31] Vulcan XC72 was provided by Cabot Company.

To manufacture the different MPLs, CNSs or Vulcan XC72 (depending on the electrodes) were deposited onto a gas diffusion media (Toray Carbon Paper -PTFE 10%, Fuel Cells Store, USA) by air-spraying a microporous ink consisting of the carbonaceous material and 10% PTFE (Teflon™ Emulsion Solution, Electrochem Inc.). After the deposition of the MPLs, sintering of the PTFE was attained by heating the electrodes at 360 °C for 30 min. For the anodic electrodes, a commercial electrode with Vulcan XC72 based MPL (Freudenberg Vliesstoffe, H23C2) was used. This procedure was used according to previous studies performed by our research group.[32,33]

Then, a platinum-based catalyst was prepared using the CNFp's as catalyst support by the Formic acid method.[34] Hexachloroplatinic acid Hexahydrated (Sygma Aldrich) was used as Platinum precursor salt. The platinum target loading was 40% wt. Then, manufactured catalyst was physicochemically analysed, in order to asseverate the correct Pt deposition on the CNFp's, resulting in a nominal Pt content of 39.8 ± 0.4% wt. (calculated by ICP) and an average Pt particle size of 3.7 ± 0.4 nm (calculated from the analysis of the TEM image shown in Figure 8). For the case of the standard Vulcan

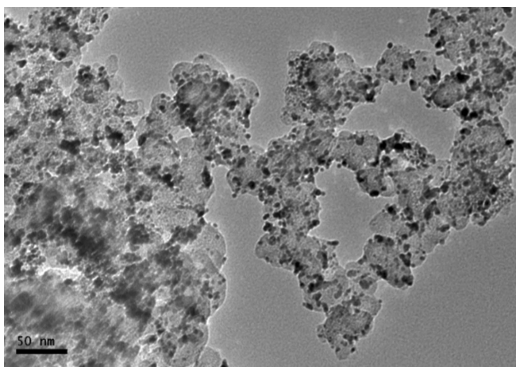

Figure 8. TEM micrographs of the Pt/CNFp catalysts.

based MEA, a commercial 40% Pt/Vulcan catalyst (provided by FuelCell Store) was used. In this case, the nominal Pt content was 40.1 ± 0.2% wt. and the average Pt particle size, 3.6 ± 1.1 nm, both parameters closely similar to the values obtained for the Pt/CNFp based catalyst. This fact means that the synthesis method used is acceptable, and it should not provide several differences, in terms of performance, due to differences on the active area of the manufactured catalyst compared with the commercial one.

Then, the different catalyst layers were deposited by spraying the catalyst ink over the electrodes. The catalyst ink for the cathodic electrodes consisted of the commercial Pt/Vulcan catalyst or the lab-made 40% wt. Pt/CNFp, PBI ionomer (1.5 wt.% PBI in N, N-dimethylacetamide, DMAc, 1–20 PBI/support ratio), and DMAc as a dispersing solvent. The Pt amount of the catalyst powder was fixed according to the results of previous studies carried out by our research group[35] and it is in agreement with the ratios used in other works shown in the literature.[36] For the anode, the commercial catalyst, Pt/Vulcan, was used in both cases. For all electrodes, the Pt loading on the two electrodes (anode and

cathode) was 0.6 mg Pt cm^{-2}. After the deposition of the catalyst layer, the electrodes were dried at 190 °C for 2 h, with the purpose of removing traces of DMAc. Then, electrodes were wetted with a solution of 10% PA and they were left to adsorb the acid for one day.

For the preparation of the MEA, a thermally treated PBI membrane (provided by Danish Power System) was doped in 85 wt.% PA for 5 days, in order to achieve good proton conductivity. The doping level acquired by the membrane was approximately 10 molecules of acid per polymer repeating unit. The thickness of the doped PBI membrane was around 82 µm. The superficial acid on the membrane was thoroughly wiped off with filter paper and the membrane was used to prepare the MEA. In order to fabricate the MEA, the doped membrane was sandwiched between a couple of electrodes and the whole system was hot-pressed at 130 °C and 1 MPa for 15 min. The completed MEA was inserted into the cell between end plates of graphite (with a five serpentine channels frame in each plate). The geometrical area of each electrode was 25 cm^2.

MEAs were mounted and characterized in a commercially available Cell Compression Unit (CCU) provided by Baltic fuel cells GmbH (Germany). The break-in procedure consists of operation at 0.1 A cm^{-2} (160 °C) and $\lambda_{H2/O2}$ excess stoichiometric coefficients of 1.5/9.0 for 70 hours. A preliminary stability test was conducted by increasing the current density to 0.3 A cm^{-2} (160 °C) and working at constant stoichiometric coefficients (λ_{H2} of 1.5 and λ_{O2} of 9.5). For further characterization, a protocol test was carried out every 48 h since the final of the break-in procedure as reported elsewhere.[36] This protocol test consisted of the following routine:

- Galvanostatic polarization curves. They were performed from the OCV to 0.40 V. First with air at constant $\lambda_{H2/air} = 1.5/2.0$ and then with oxygen at constant $\lambda_{H2/O2} = 1.5/9.5$.
- Electrochemical impedance spectroscopy (EIS) tests. The EIS tests were performed at 0.10 A cm^{-2} with 10 mV AC perturbation amplitude and frequency range from 100 kHz to 100 mHz. This sequence of EIS tests was carried out with air as oxidant and then, the same procedure was repeated with oxygen.
- Cyclic voltammetries (CV). The cathode side was purged with nitrogen and hydrogen flowed through anode side with flows of 0.1/0.1 L min^{-1} H_2/N_2. The CV was carried out from 0.05 V to 1.00 V with a scan rate of 100 mV s^{-1}. Then, the electrochemical surface area (ECSA) of cathode was estimated.

Operation conditions changes abruptly during this protocol test, and the usage of pure oxygen as oxidant increase the degradation of the system, making more useful the stability data obtained from these short time experiments. It must be pointed out that during this period, the systems underwent more aggressive operational conditions, with six electrochemical characterization tests. This operational mode is expected to produce a faster degradation, as compared with similar studies of HT-PEMFCs, for which no characterization protocols are performed during the lifetests or they are performed in longer periods of time (f.i. every 200 hours approx.).[29,37–39]

To the best of our knowledge, in the literature there are not described any single cell operation with PBI-based HT-PEMFC systems, where these new micro porous layer (MPL) and catalyst supports are used at the same time in the cathode. Just a preliminary test was performed by our research group testing the CNSs based MPL in a lifetest, but with a lesser aggressive operational conditions.[31] It means that results obtained cannot be compared with any other previous value and it is the comparison among them, the most valuable result expected, rather than the particular values reached in any parameter. For this reason, special care was taken during the experiments and they were carried out using the same cell and were planned for the same operation conditions in order to have comparable results.

Acknowledgements

The authors thank the European Commission as this work was supported by the Seventh Framework Programme through the project CISTEM (FCH-JU Grant Agreement Number 325262). The authors are grateful to Danish Power System for providing the PBI-based membranes.

Conflict of Interest

The authors declare no conflict of interest.

Keywords: carbon nanostructures · electrocatalysts · fuel cells · microporous layer · stability

[1] S. S. Araya, F. Zhou, V. Liso, S. L. Sahlin, J. R. Vang, S. Thomas, X. Gao, C. Jeppesen, S. Knudsen Kær, *Int. J. Hydrogen Energy* **2016**, *41*, 21310–21344.
[2] J. B. d'Arbigny, G. Taillades, M. Marrony, D. J. Jones, J. Rozie're, *Chem. Commun.* **2011**, *47*, 7950–7952.
[3] Y. Zhang, S. Chen, Y. Wang, W. Ding, R. Wu, L. Li, X. Qi, Z. Wei, *J. Power Sources* **2015**, *273*, 62–69.
[4] M. Ahn, Y.-H. Cho, Y.-H. Cho, J. Kim, N. Jung, Y.-E. Sung, *Electrochim. Acta* **2011**, *56*, 2450–2457.
[5] A. Chandan, M. Hattenberger, A. El-kharouf, D. Shangfeng, A. Dhir, V. Self, B. G. Poller, A. Ingram, W. Bujalski, *J. Power Sources* **2013**, *231*, 264–278 .
[6] Q. Li, J. O. Jensen, R. F. Savinell, N. J. Bjerrum, *Progress in Polymer Science (Oxford)* **2009**, *34*, 449–477.
[7] N. Üregen, K. Pehlivanoglu, Y. Özdemir, Y. Devrim, *Int. J. Hydrogen Energy* **2017**,*42*, 2636–2647.
[8] J. Lobato, P. Cañizares, M. A. Rodrigo, D. Úbeda, F. J. Pinar. *ChemSusChem* **2011**, *4*, 1489–1497.
[9] Y. Park, K. Kakinuma, M. Uchida, H. Uchida, M. Watanabe, *Electrochim. Acta* **2014**, *123*, 84–92.
[10] N. Linse, G. G. Scherer, A. Wokaun, L. Gubler, *J. Power Sources* **2012**, *219*, 240–248.
[11] J. H. Park, S. D. Yima, T. Kim, S. Park, Y. Yoon, G. Park, T. Yang, E. Park, *Electrochim. Acta* **2012**, *83*, 294–304.
[12] R. Borup, J. Meyers, B. Pivovar, Y. S. Kim, R. Mukundan, N. Garland, D. Myers, M. Wilson, F. Garzon, D. Wood, P. Zelenay, K. More, K. Stroh, T. Zawodzinski, J. Boncella, J. E. McGrath, M. Inaba, K. Miyatake, M. Hori, K. Ota, Z. Ogumi, S. Miyata, A. Nishikata, Z. Siroma, Y. Uchimoto, K. Yasuda, K. Kimijima, N. Iwashita, *Chem. Rev.* **2007**, *107*, 3904–3951.
[13] L. M. Roen, C. H. Paik, T. D. Jarvi, Electrochem. *Solid-State Lett.* **2004**, *7*, A19–A22.
[14] S. Zhang, X.-Z Yuan, J. N. C. Hin, H. Wang, K. A. Friedrich, M. Schulze, *J. Power Sources* **2009**, *194*, 588–600.
[15] H. Zamora, P. Cañizares, M. A. Rodrigo, J. Lobato, *Fuel Cells* **2015**, *15*, 375–383.
[16] F. N. Büchi. M. Inaba, T. J. Schmidt, *Polymer Electrolyte Fuel Cell Durability, Springer Science+Business Media, LLC*, **2009** DOI: 10.1007/978-0-387-85536-3.
[17] R. Dhiman, E. Johnson, E. M. Skou, P. Morgen, S. M. Andersen, *J. Mater. Chem. A* **2013**, *1*, 6030–6036.
[18] S. N. Stamatin, J. Speder, R. Dhiman, M. Arenz, E. M. Skou, *ACS Appl. Mater. Interfaces* **2015**, *7*, 6153–6161.
[19] B. Avasarala, T. Murray, W. Li, P. Haldar, *J. Mater. Chem.* **2009**, *19*, 1803–1805.
[20] S.-Y Huang, P. Ganesan, S. Park, B. N. Popov, *J. Am. Chem. Soc.* **2009**, *131*, 13898–13899.

[21] S. Sharma, B. G. Pollet, *J. Power Sources* **2012**, *208*, 96–119.
[22] L. Qu, Y. Liu, J. B. Baek, L. Dai, *ACS Nano* **2010**, *4*, 1321.
[23] D. Sebastián, I. Suelves, R. Moliner, M. J. Lázaro, A. Stassi, V. Baglio, A. S. Aricò, *Appl. Catal. B* **2013**, *132–133*, 22–27.
[24] V. Jimenez, A. Nieto-Marquez, J. A. Díaz, R. Romero, P. Sánchez, J. L. Valverde, A. Romero, *Ind. Eng. Chem. Res.* **2009**, *48*, 8407–8417.
[25] A. Nieto-Márquez, I. Espartero, J. Lazo, A. Romero, J. L. Valverde, *Chem. Eng. J.* **2009**, *153*, 211–216.
[26] F. J. Pinar, P. Cañizares, M. A. Rodrigo, D. Úbeda, J. Lobato, *J. Power Sources* **2015**, *274*, 177–185.
[27] S. J. Andreasen, J. L. Jespersen, E. Schaltz, S. K. Kær, *Fuel Cells* **2009**, *09*, 463–473.
[28] J. L. Jespersen, E. Schaltz, S. K. Kær, *J. Power Sources* **2009**, *191*, 289–296.
[29] F. J. Pinar, N. Pilinski, P. Wagner, *AIChE Journal*, **2015**, *62*, 1, 217–227.
[30] C. Y. Chen, W. H. Lai, *J. Power Sources* **2010**, *195*, 7152–7159.
[31] H. Zamora, P. Cañizares, J. Plaza, M. A. Rodrigo, J. Lobato, *ChemSusChem* **2016**, *9*, 1187–1193.
[32] J. Lobato, H. Zamora, P. Cañizares, J. Plaza, M. A. Rodrigo, *J. Power Sources* **2015**, *288*, 288–295.
[33] J. Lobato, P. Cañizares, M. A. Rodrigo, D. Úbeda, F. J. Pinar, J. J. Linares, *Fuel Cells* **2010**, *10*, 770–777.
[34] F. Colmati, E. Antolini, E. R. Gonzalez, *Electrochim. Acta* **2005**, *50*, 5496–5503.
[35] J. Lobato, P. Cañizares, M. A. Rodrigo, J. J. Linares, D. Úbeda, F. J. Pinar, *Fuel Cells* **2010**, *10*, 312–319.
[36] A. S. Pushkarev, I. V. Pushkareva, S. A. Grigoriev, V. N. Kalinichenko, M.Yu. Presniakov, V. N. Fateev, *Int. J. Hydrogen Energy* **2015**, *40*, 14492–14497.
[37] F. J. Pinar, N. Pilinski, M. Rastedt, P. Wagner, *Int. J. Hydrogen Energy* **2015**, *40*, 5432–5438.
[38] R. Kerr, H. R. García, M. Rastedt, P. Wagner, S. M. Alfaro, M. T. Romero, C. Terkelsen, T. Steenberg, H. A. Hjuler, *Int. J. Hydrogen Energy* **2015**, *40*, 16860–16866.
[39] G–B. Jung, K–Y. Chuang, T–C. Jao, C–C. Yeh, C–Y. Lin. *Applied Energy* **2012**, *100*, 81–86.

Manuscript received: July 12, 2017
Accepted Article published: September 18, 2017
Version of record online: October 5, 2017